# Intraday Repeatability of Bruch's Membrane Opening-Based Neuroretinal Rim Measurements

Philip Enders, Andreas Bremen, Friederike Schaub, Manuel M. Hermann, Michael Diestelhorst, Thomas Dietlein, Claus Cursiefen, and Ludwig M. Heindl

Department of Ophthalmology, University Hospital of Cologne, Cologne, Germany

Correspondence: Philip Enders, Department of Ophthalmology, University of Cologne, Kerpener Strasse 62, 50924 Cologne, Germany; philip.enders@uk-koeln.de.

Submitted: August 15, 2017
Accepted: September 14, 2017

Citation: Enders P, Bremen A, Schaub F, et al. Intraday repeatability of Bruch's membrane opening-based neuroretinal rim measurements. *Invest Ophthalmol Vis Sci*. 2017;58:5195–5200. DOI:10.1167/iovs.17-22812

**Purpose.** To assess possible intraday variability in Bruch's membrane opening–based (BMO) assessment of neuroretinal rim by spectral-domain optical coherence tomography (SD-OCT) of the optic nerve head (ONH) as well as to evaluate its independence from intraindividual IOP changes.

**Methods.** In this noninterventional, prospective cohort study, 51 consecutively enrolled patients with glaucoma or ocular hypertension underwent standardized SD-OCT of the ONH and IOP assessment at two different time points with a time gap of 5 hours on the same day. Random effects models, intraclass correlation coefficients (ICC) and Bland-Altman plots were used to analyze repeatability of BMO minimum rim width (BMO-MRW) and area (BMO-MRA) and peripapillary retinal nerve fiber layer (RNFL) thickness measurements.

**Results.** Mean BMO area was 1.86 ± 0.30 $mm^2$. At baseline, mean BMO-MRW was 206.46 ± 0.86 µm, mean BMO-MRA was 0.89 ± 0.34 $mm^2$, and mean RNFL thickness was 71.61 ± 0.20 µm. Within intraindividual measurements, mean difference was 2.95 µm or 1.76% for BMO-MRW, 0.02 $mm^2$ or 2.68% for BMO-MRA, and 1.18 µm or 1.89% for RNFL thickness. Comparing time points, $\eta^2$ was 0.001 ($P = 0.757$) for RNFL thickness, 0.043 ($P = 0.01$) for BMO-MRA, and 0.07 ($P = 0.06$) for BMO-MRW. Intraclass correlation coefficients were greater than 0.994, respectively. Variability of morphometric parameters did not correlate to intraindividual IOP fluctuations.

**Conclusions.** Assessment of BMO-MRW by SD-OCT shows high intraday repeatability, which is comparable to the parameter RNFL thickness. Variability seems not to be driven by typical moderate intraday fluctuations of IOP. The two-dimensional parameter BMO-MRA incorporates a fairly higher intraindividual variability.

Keywords: Bruch's membrane opening-based neuroretinal rim measurements, inter-measurement variation analysis, SD-OCT of the optic nerve head

Spectral-domain optical coherence tomography (SD-OCT) of the optic nerve head (ONH) becomes more and more the current gold standard for morphometric assessment in glaucoma diagnostics and follow-up.[1] This technique excels previous approaches as confocal scanning laser tomography by a superior diagnostic power to detect glaucoma and relative observer independency.[1–3] Retinal structures between Bruch's membrane opening (BMO) and the internal limiting membrane (ILM) are assessed. Additionally, subsurface structures are analyzed.[1,4–11] Correlation of morphometric parameters of the ONH and visual field function has been evaluated in several studies.[1,12–22] In addition to the clinically available parameters Bruch's membrane opening–based minimal rim width (BMO-MRW) and peripapillary retinal nerve fiber layer (RNFL) thickness, two studies on the two dimensional parameter Bruch's membrane opening minimal rim area (BMO-MRA) showed high diagnostic power for all ONH sizes and equalized differences in BMO-MRW between very large and very small ONHs.[1,23]

As follow-up data become available, first studies were conducted to assess the performance of SD-OCT for detection of progression of glaucomatous damage to the ONH. Those studies have shown a relative superiority for the parameter RNFL thickness over rim-based parameters.[24] One hypothesis for this finding was the presence of intraday fluctuations of anatomic ONH structures due to vascular and intraocular as intrathecal pressure changes. While some studies focused on the consistency of BMO detection, it was unclear whether intraday changes in parameters depending on the examination time were present.[24]

In the present study, we prospectively recruited a cohort of 51 patients with glaucoma or suspicion of glaucoma, which were hospitalized for 24-hour IOP measurements to compare two SD-OCT examinations of the ONH with a time difference of 5 hours on the same day.

## Methods

Data for this single-center, prospective study were acquired from October to December 2016 at the Department of Ophthalmology, University Hospital of Cologne, Germany. Patients received SD-OCT measurements of the ONH at two different time points on the same day. The first examination was conducted during the late morning between 11:00 AM and 12:00 PM, while the second examination took place around 5

PM. In several participants, an additional third SD-OCT measurement had been acquired during clinical routine 24 hours before the first study assessment. Intraocular pressure was measured by corneal rebound tonometry directly before every SD-OCT examination was initiated (Icare tonometer TA01i; Icare Finland Oy, Vantaa, Finland).[25–27]

## Inclusion and Exclusion Criteria

Inclusion criteria were hospitalization for 24-hour IOP measurement due to presence of glaucoma or suspicion of glaucoma in clinical assessment. Written informed consent was obtained from all participants. Only examinations with an image quality index of greater than 15 dB were included in the analysis. Exclusion criteria were insufficiency of clear optical media defined by the ability to reach a sufficient SD-OCT quality index as defined, retinal, or other pathology presenting any potential bias for imaging analysis (e.g., ONH drusen, peripapillary choroidal neovascularization, significant epiretinal membrane), inability for accurate fixation, recent intraocular surgery (<7 days), or other causes for hospitalization than defined within the inclusion criteria.

Participants' eyes were classified into three groups according to their peripapillary global RNFL thickness to reflect the degree of damage in neuroretinal tissue. Normal global RNFL was defined as thickness of larger than 85 μm. Moderate damage was defined as thinning of RNFL to 65 to 84 μm, while severe damage was indicated by a global RNFL thickness of less than 64 μm.

## Morphometric Analyses of the Optic Disc

Spectral-domain OCT examinations were performed by Spectralis SD-OCT (Heidelberg Engineering GmbH, Heidelberg, Germany) according to standard operating and imaging procedures using a light source of 870 nm. Included OCT data comprised an image quality index of greater than 15 dB. The scanning pattern was centered on the BMO with radial equidistance (24-high resolution 15° radial scans, each averaged from 27 B-scans). The examiners controlled the centration of the scan to the optic disc and corrected errors in detection of ILM and BMO. Two reviewers assessed independently especially those cases with discrepancies between measurements to exclude bias by manual correction. Optical coherence tomography–based parameters BMO-MRW and BMO area as well as RNFL thickness were calculated by the device operating software tool provided by Heidelberg Engineering, including a data export batch provided by the manufacturer. Bruch's membrane opening MRA calculation was performed by Heidelberg Engineering software Spectralis SP-X VWM. Gardiner and associates[1] proposed the principle of BMO-MRA calculation.

## Ethics and Statistics

Formal approval to conduct this study was obtained from the Ethics Committee of the University of Cologne (No. 16-340). Written informed consent has been obtained of all participants prior to additional SD-OCT and IOP assessments. All tenets of the Declaration of Helsinki have been regarded. Statistical analyses were performed by SPSS (version 22.0; IBM Corp. Armonk, NY, USA). Differences between time points and differences between absolute relative changes of MRW, MRA, and RNFL were examined using random effects models. Type A intraclass correlation coefficients (ICC) as well as Bland-Altman plots were used. Spearman's rank correlation analysis was used to test for correlation between morphometric parameters and IOP. The threshold for statistical significance was $P$ less than 0.05

**Table 1.** Baseline Data and Optic Nerve Head Morphometrics

| Time of Examination | First Examination | Second Examination |
|---|---|---|
| Mean ± SD | 11:32 ± 0:23 | 16:52 ± 0:26 |
| Sex, *n* (%) | | |
| Men | 45 (46.4) | – |
| Women | 52 (53.6) | |
| Age, y | | |
| Mean ± SD | 63.6 ± 15.5 | – |
| Median | 67.2 | |
| Eye, *n* (%) | | |
| Right | 48 (49.5) | – |
| Left | 49 (50.5) | |
| Lens status (%) | | |
| Phakic | 62 | |
| Pseudophakic | 35 | |
| Uncorrected refractive error, $n = 69$, D | | |
| Spherical equivalent (SE) | −0.55 ± 2.94 | |
| Range | −8.00 to +6.4 | |
| Number of patients exceeding SE of ±5.0 D (*n*) | 6 | |
| Current refractive error (scan focus, D) | | |
| Mean ± SD | −0.80 ± 1.36 | – |
| IOP, mm Hg | | |
| Mean ± SD | 14.5 ± 4.8 | 13.8 ± 3.7 |
| Mean global BMO area, $mm^2$ | | |
| Mean ± SD | 1.86 ± 0.30 | 1.86 ± 0.31 |
| Mean global BMO-MRW, μm | | |
| Mean ± SD | 206.46 ± 85.88 | 205.24 ± 85.71 |
| Mean global BMO-MRA, $mm^2$ | | |
| Mean ± SD | 0.89 ± 0.03 | 0.88 ± 0.03 |
| Mean global RNFL thickness, μm | | |
| Mean ± SD | 71.61 ± 19.64 | 71.56 ± 19.45 |

D, diopters.

# Results

In this prospective study, 51 patients were enrolled, whereof 97 eyes could be included in the analyses. In five eyes of these patients, insufficient image quality (four eyes) or data acquisition errors (one eye) led to exclusion. Epidemiology and baseline data are summarized in Table 1.

In all included eyes, mean BMO area was 1.86 ± 0.30 $mm^2$. The first SD-OCT examination was conducted in average at 11:32 AM (range, 10:58 AM to 12:45 PM), the second examination at 4:54 PM (range, 4 to 5:50 PM) resulting in a mean interval of 5.4 hours. Mean BMO-MRW in the first examination was 206.46 ± 0.86 μm (range, 50.26–508.38 μm), mean BMO-MRA was 0.89 ± 0.34 $mm^2$ (range, 0.28–1.94 $mm^2$), and mean RNFL thickness was 71.61 ± 0.20 μm (range, 34–111 μm).

At the second SD-OCT examination, mean BMO-MRW was 205.24 ± 0.86 μm (range, 54.78–501.03 μm), mean BMO-MRA

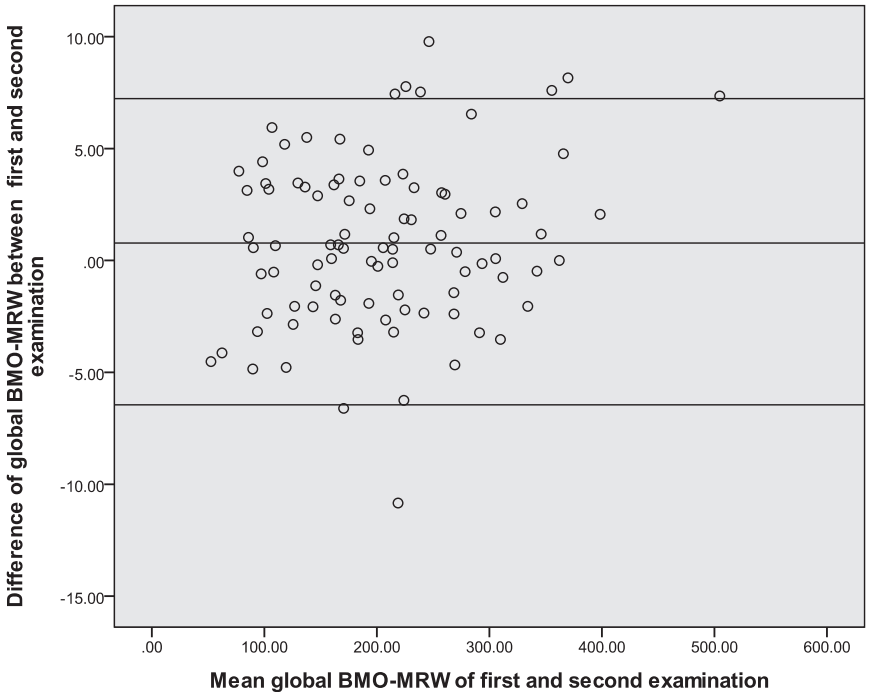


Figure 1. Bland-Altmann plot for intraday repeatability of BMO-MRW measurements.

was 0.88 ± 0.34 mm$^2$ (range, 0.30–1.88 mm$^2$), and mean RNFL thickness was 71.56 ± 0.19 μm (range, 34–111 μm).

## Repeatability Analyses of Morphometric Intraday Measurements

Mean difference between absolute intraindividual measurements was 2.95 μm or 1.76% for BMO-MRW, 0.02 mm$^2$ or 2.68% for BMO-MRA, and 1.18 μm or 1.89% for RNFL thickness. While BMO-MRW and RNFL thickness demonstrated a comparable relative change between intraday measurements ($P$ = 0.45), BMO-MRA showed significantly higher intraindividual variability compared with BMO-MRW ($P < 0.001$) and RNFL thickness ($P = 0.008$). Comparison of time points resulted in $\eta^2 = 0.001$ with $P = 0.757$ for RNFL thickness, $\eta^2 = 0.04$ with $P = 0.06$ for BMO-MRW, and $\eta^2 = 0.07$ with $P = 0.01$ for BMO-MRA. Figures 1 through 3 show Bland-Altman plots for graphical display of intraday repeatability of the three morphometric

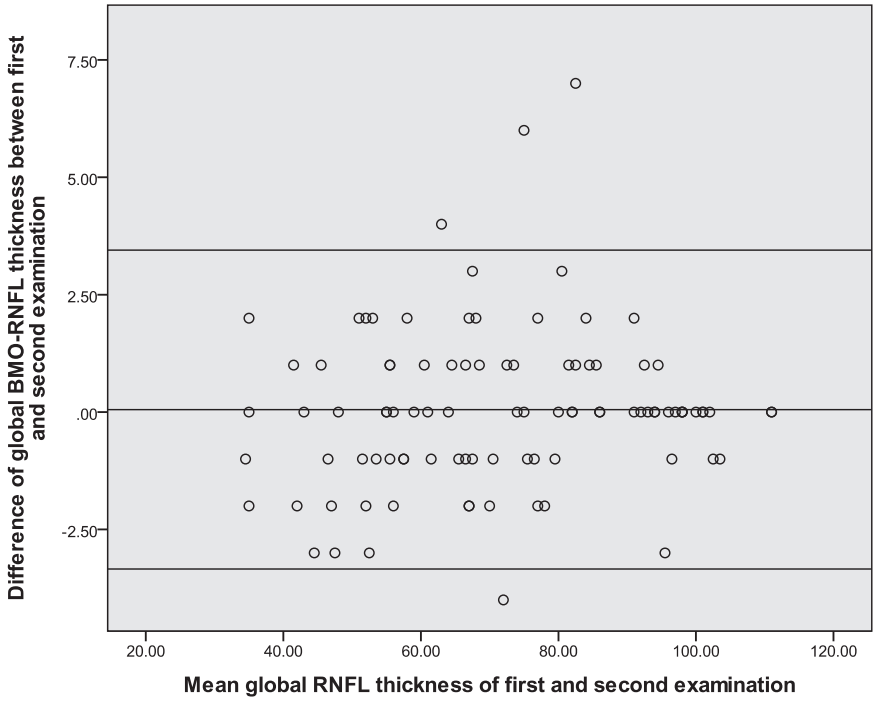


Figure 2. Bland-Altmann plot for intraday repeatability of RNFL thickness measurements.

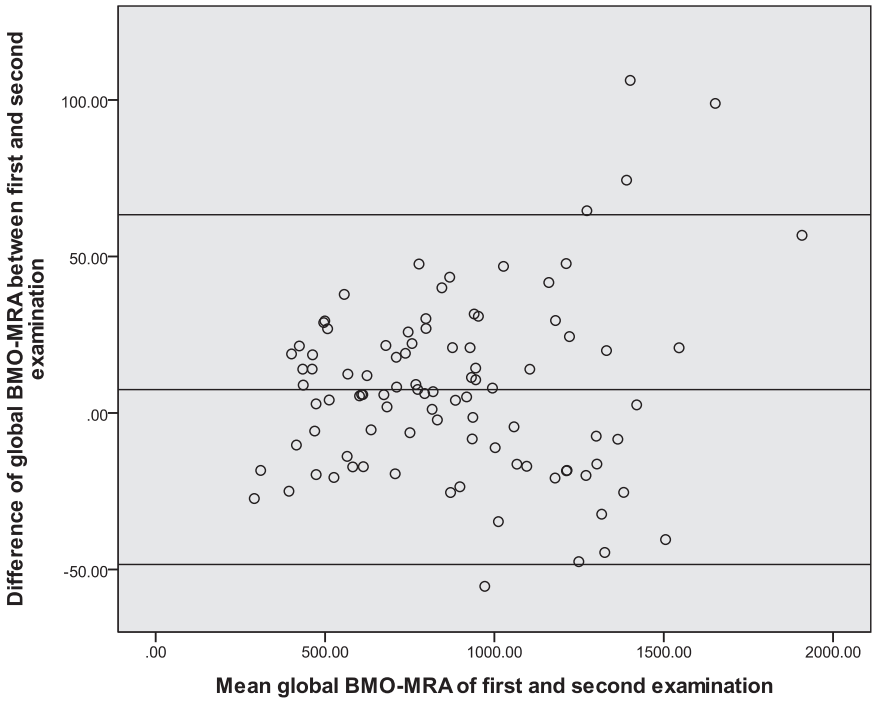


FIGURE 3. Bland-Altmann plot for intraday repeatability of BMO-MRA measurements.

parameters. Intraclass correlation coefficients 95% confidence intervals (CI) were 0.994 to 0.997 for RNFL thickness ($P < 0.001$), 0.999 to 1.0 for BMO-MRW ($P < 0.001$), and 0.994 to 0.998 for BMO-MRA ($P < 0.001$).

## Reproducibility of SD-OCT Segmentation and Intraday IOP Measurements

In 55 of 97 eyes, ILM and BMO detection was highly reproducible. In those eyes, manual correction of ILM or BMO was necessary in only less than three of 24 scans. In this group, mean differences between absolute intraindividual measurements of all the parameters were not different from those of the entire cohort. Regarding BMO correction solely, 80.4% of all eyes included in this study had equal or less than 8 scans with BMO corrections in two examinations, resulting in less than four corrections per examination. Additionally, results for parameters BMO area and BMO-MRW were compared with and without manually correction. In all eyes included, mean corrected BMO area was 1.865 ± 0.30 $mm^2$ in the morning and 1.861 ± 0.31 $mm^2$ in the evening resulting in a difference of 0.004 $mm^2$. Mean uncorrected BMO area was 1.839 ± 0.31 $mm^2$ and 1.830 ± 0.32 $mm^2$ respectively, resulting in a difference of 0.009 $mm^2$.

Mean IOP was 14.49 mm Hg (range, 7–31 mm Hg) at the first and 13.77 mm Hg (range, 7–22 mm Hg) at the second examination. Intraindividual absolute mean change of IOP between the two measurements was 2.7 mm Hg. Intraindividual variability in morphometric parameters did not correlate significantly with intraindividual changes of IOP (rho = 0.1–0.2; $P > 0.12$).

## Repeatability Analysis According to Peripapillary Global RNFL Thickness Subgroups

Global RNFL thickness in the first measurement was larger than 85 μm in 29 eyes, between 65 and 84 μm in 32 eyes and less than 64 μm. Between those groups, relative change between intraday measurements increased toward higher degree of ONH damage, for BMO-MRW from 1.2% to 2.4% ($P = 0.05$), for RNFL thickness from 0.9% to 2.5% ($P < 0.001$), and for BMO-MRA from 2.4% to 3.0% ($P = 0.59$).

## Supplemental Examination With a 24-Hour Time Gap

In 48 eyes, a third SD-OCT examination was conducted within clinical routine diagnostics for glaucoma evaluation with a

TABLE 2. Intraclass Correlation Coefficients Between Intraday Measurements

| Intraclass Correlation Coefficients | BMO-MRW | BMO-MRA | RNFL Thickness |
|---|---|---|---|
| Global | 0.999 (0.999–0.999) | 0.996 (0.994–0.998) | 0.996 (0.994–0.997) |
| Temporal sector | 0.996 (0.994–0.997) | 0.993 (0.990–0.996) | 0.991 (0.987–0.994) |
| Temporal superior sector | 0.996 (0.995–0.998) | 0.990 (0.985–0.994) | 0.993 (0.990–0.996) |
| Temporal inferior sector | 0.996 (0.994–0.997) | 0.992 (0.988–0.995) | 0.995 (0.993–0.997) |
| Nasal sector | 0.998 (0.996–0.998) | 0.995 (0.992–0.996) | 0.983 (0.974–0.989) |
| Nasal superior sector | 0.996 (0.994–0.997) | 0.989 (0.984–0.993) | 0.984 (0.976–0.989) |
| Nasal inferior sector | 0.995 (0.992–0.996) | 0.989 (0.983–0.993) | 0.942 (0.914–0.961) |

Values represent the mean and 95% CI.

mean interval of 22.9 hours before or after the first study examination in average at 11:54 AM in the morning hours.

Mean BMO-MRW in this supplemental examination was 216.46 ± 0.35 μm (range, 52.25–404.05 μm), mean BMO-MRA was 0.91 ± 0.33 $mm^2$ (range, 0.28–1.63 $mm^2$), and mean RNFL thickness was 74.74 ± 0.20 μm (range, 36–102 μm).

For intraindividual measurements, mean difference of absolute values between the supplemental examination and the first examination of the study was 3.74 μm or 2.14% for BMO-MRW, 0.03 $mm^2$ or 3.19% for BMO-MRA, and 2.07 μm or 3.22% for RNFL thickness. Proportional frequency in relative change between measurements was lower for BMO-MRW compared with BMO-MRA ($P = 0.008$) and to RNFL thickness ($P = 0.12$).

Results of random effects models with repeated measures did not reach the defined level for statistical significance.

## Discussion

Morphometric assessment of the ONH by SD-OCT has become a cornerstone in glaucoma diagnostics and follow-up. Diagnostic power to detect and differentiate glaucomatous damage in a single observation has been analyzed in numerous studies for a broad range of clinical and anatomic situations.[8–10]

As follow-up data after introduction of this technique become more and more available, first results seem to demonstrate a superior correlation of peripapillary RNFL thickness to functional loss in visual field testing compared with BMO-based parameters. A possible explanation of this inferiority of BMO-based parameters to detect change was thought in a higher variability of measurements due to fluctuations in anatomic ONH structures. Consistency of BMO detection of the ONH in Cirrus SD-OCT was evaluated by Hwang and associates,[28] who found overall satisfactory consistency levels and higher discrepancies in myopic eyes with peripapillary atrophy. In another study of Pearce et al.,[29] intervisit test-retest variability of OCT in glaucoma was excellent for horizontal and vertical cup/disc ratios and ganglion cell complex. Mansouri et al.[30] reported good correlations between OCT measurements in sitting and supine positions and high repeatability of measurements of ONH and RNFL.

In this study, we could show that BMO-MRW and RNFL thickness parameters show a high degree of consistency between measurements in the morning and in the afternoon. Relative change of absolute differences between examinations in these two standard parameters does not show a statistically significant difference, ICC, and Bland-Altman plots support this conclusion. BMO-based minimum rim area (BMO-MRA) has been proposed as an additional, three-dimensional parameter to measure the neuroretinal rim by SD-OCT.[1,12] Bruch's membrane opening MRA has been shown to offer higher comparability between differences in ONH sizes. Bruch's membrane opening MRA showed a significantly higher relative intraindividual variability between both examinations on the same day. As BMO area measurements were stable, reason for this might be the more complex calculation algorithm of this two-dimensional parameter with independent localized minimization of 48 trapezoids.

Toward progressive damage of neuroretinal tissues, we did find a slight but significant increase in variability between intraday measurements. This increase was statistically significant for BMO-MRW and RNFL thickness parameters. A reason for this might be the device-specific variation, which is constant for all measurements but gains relative relevance when morphometric parameters worsen. Changes in IOP could represent an additional factor influencing ONH morphology analyzed by SD-OCT. In our study, intraday IOP fluctuations were moderate between both measurements. The effects of higher changes in IOP on morphology, for example, before and after trabeculectomy, remain unclear and should be focus on an additional study.

Incorrect automated detection of ILM or BMO structures by the operating software requiring consecutive manual correction might represent another reason for intraindividual variation between two measurements. In our study, manual correction of Bruch's membrane ending had an effect on the BMO area size but seemed not to have affected the parameter BMO-MRW. It is not surprising that BMO area size is affected by manual correction, as the calculation algorithms tend to face difficulties in detection of Bruch's membrane ending when border tissue of Elschnig is present in peripapillary atrophy. In consequence, true BMO area is larger than measured by the automated algorithm. Intraday variability between the two measurements was at the same level regardless of whether BMO correction was applied or not.

Variation in vascular components of the analyzed anatomic structured might also be responsible for intraindividual variation in measurements. That question was not in scope of our study. Future studies assessing vascular parameters (e.g., blood pressure, choroidal thickness, vascular density in Angio-OCT) need to be undertaken.

Limitations to the study are the missing information on the original refractive status prior to cataract surgery in 30% of the patients and the absence of axial length measurements in all eyes. For future studies, obtaining this information in all patients would be desirable.

To summarize the main conclusions of the present study, we did not find any relevant intraday variability in SD-OCT based morphometric parameters between measurements taken with a time gap of 5 hours. Intraclass correlation coefficients levels were excellent. Variations in diagnostic power to detect progression between BMO-based parameters and peripapillary rim measurements seem not to be driven by intraday fluctuations of ONH morphology or by changes in IOP.

### Acknowledgments

The authors thank the associated statistician of our group, Werner Adler (University of Erlangen) for his support to calculate random effects models. They also thank all technical experts of our imaging laboratory and well as FOR 2240 "(Lymph-) Angiogenesis And Cellular Immunity In Inflammatory Diseases Of The Eye" for their support.

Disclosure: **P. Enders**, None; **A. Bremen**, None; **F. Schaub**, None; **M.M. Hermann**, None; **M. Diestelhorst**, None; **T. Dietlein**, None; **C. Cursiefen**, None; **L.M. Heindl**, None

### References

1. Gardiner SK, Ren R, Yang H, Fortune B, Burgoyne CF, Demirel S. A method to estimate the amount of neuroretinal rim tissue in glaucoma: comparison with current methods for measuring rim area. *Am J Ophthalmol*. 2014;157:540–549.e2.
2. Reis AS, O'Leary N, Yang H, et al. Influence of clinically invisible, but optical coherence tomography detected, optic disc margin anatomy on neuroretinal rim evaluation. *Invest Ophthalmol Vis Sci*. 2012;53:1852–1860.
3. Reis AS, Sharpe GP, Yang H, Nicolela MT, Burgoyne CF, Chauhan BC. Optic disc margin anatomy in patients with glaucoma and normal controls with spectral domain optical coherence tomography. *Ophthalmology*. 2012;119:738–747.
4. Povazay B, Hofer B, Hermann B, et al. Minimum distance mapping using three-dimensional optical coherence tomography for glaucoma diagnosis. *J Biomed Opt*. 2007;12:041204.

5. Abramoff MD, Lee K, Niemeijer M, et al. Automated segmentation of the cup and rim from spectral domain OCT of the optic nerve head. *Invest Ophthalmol Vis Sci*. 2009;50:5778–5784.
6. Mwanza JC, Oakley JD, Budenz DL, Anderson DR; for the Cirrus Optical Coherence Tomography Normative Database Study Group. Ability of cirrus HD-OCT optic nerve head parameters to discriminate normal from glaucomatous eyes. *Ophthalmology*. 2011;118:241–248.e1.
7. Chen TC. Spectral domain optical coherence tomography in glaucoma: qualitative and quantitative analysis of the optic nerve head and retinal nerve fiber layer (an AOS thesis). *Trans Am Ophthalmol Soc*. 2009;107:254–281.
8. Chauhan BC, Burgoyne CF. From clinical examination of the optic disc to clinical assessment of the optic nerve head: a paradigm change. *Am J Ophthalmol*. 2013;156:218–227.e2.
9. Chauhan BC, Danthurebandara VM, Sharpe GP, et al. Bruch's membrane opening minimum rim width and retinal nerve fiber layer thickness in a normal white population: a multicenter study. *Ophthalmology*. 2015;122:1786–1794.
10. Chauhan BC, O'Leary N, Almobarak FA, et al. Enhanced detection of open-angle glaucoma with an anatomically accurate optical coherence tomography-derived neuroretinal rim parameter. *Ophthalmology*. 2013;120:535–543.
11. Bowd C, Zangwill LM, Medeiros FA, et al. Structure-function relationships using confocal scanning laser ophthalmoscopy, optical coherence tomography, and scanning laser polarimetry. *Invest Ophthalmol Vis Sci*. 2006;47:2889–2895.
12. Muth DR, Hirneiss CW. Structure-function relationship between Bruch's membrane opening-based optic nerve head parameters and visual field defects in glaucoma. *Invest Ophthalmol Vis Sci*. 2015;56:3320–3328.
13. Gardiner SK, Johnson CA, Cioffi GA. Evaluation of the structure-function relationship in glaucoma. *Invest Ophthalmol Vis Sci*. 2005;46:3712–3717.
14. Anton A, Yamagishi N, Zangwill L, Sample PA, Weinreb RN. Mapping structural to functional damage in glaucoma with standard automated perimetry and confocal scanning laser ophthalmoscopy. *Am J Ophthalmol*. 1998;125:436–446.
15. Anderson RS. The psychophysics of glaucoma: improving the structure/function relationship. *Prog Retin Eye Res*. 2006;25:79–97.
16. Caprioli J. Correlation of visual function with optic nerve and nerve fiber layer structure in glaucoma. *Surv Ophthalmol*. 1989;33(Suppl):319–330.
17. Garway-Heath DF, Holder GE, Fitzke FW, Hitchings RA. Relationship between electrophysiological, psychophysical, and anatomical measurements in glaucoma. *Invest Ophthalmol Vis Sci*. 2002;43:2213–2220.
18. Harwerth RS, Carter-Dawson L, Smith EL III, Crawford ML. Scaling the structure–function relationship for clinical perimetry. *Acta Ophthalmol Scand*. 2005;83:448–455.
19. Enders P, Schaub F, Hermann MM, Cursiefen C, Heindl LM. Neuroretinal rim in non-glaucomatous large optic nerve heads: a comparison of confocal scanning laser tomography and spectral domain optical coherence tomography. *Br J Ophthalmol*. 2017;101:138–142.
20. Schlottmann PG, De Cilla S, Greenfield DS, Caprioli J, Garway-Heath DF. Relationship between visual field sensitivity and retinal nerve fiber layer thickness as measured by scanning laser polarimetry. *Invest Ophthalmol Vis Sci*. 2004;45:1823–1829.
21. Enders P, Schaub F, Adler W, Nikoluk R, Hermann MM, Heindl LM. The use of Bruch's membrane opening-based optical coherence tomography of the optic nerve head for glaucoma detection in microdiscs. *Br J Ophthalmol*. 2017;101:530–535.
22. Enders P, Schaub F, Heindl LM. Spectral-domain optical coherence tomography-derived characteristics of bruch membrane opening in a young adult australian population. *Am J Ophthalmol*. 2017;174:178–179.
23. Enders P, Adler W, Schaub F, et al. Novel Bruch's membrane opening minimum rim area equalizes disc size dependency and offers high diagnostic power for glaucoma. *Invest Ophthalmol Vis Sci*. 2016;57:6596–6603.
24. Gardiner SK, Demirel S, Reynaud J, Fortune B. Changes in retinal nerve fiber layer reflectance intensity as a predictor of functional progression in glaucoma. *Invest Ophthalmol Vis Sci*. 2016;57:1221–1227.
25. Gao F, Liu X, Zhao Q, Pan Y. Comparison of the iCare rebound tonometer and the Goldmann applanation tonometer. *Exp Ther Med*. 2017;13:1912–1916.
26. Kato Y, Nakakura S, Matsuo N, et al. Agreement among Goldmann applanation tonometer, iCare, and Icare PRO rebound tonometers; non-contact tonometer; and Tonopen XL in healthy elderly subjects [published online ahead of print April 9, 2017]. *Int Ophthalmol*. doi:10.1007/s10792-017-0518-2.
27. Salim S, Du H, Wan J. Comparison of intraocular pressure measurements and assessment of intraobserver and interobserver reproducibility with the portable ICare rebound tonometer and Goldmann applanation tonometer in glaucoma patients. *J Glaucoma*. 2013;22:325–329.
28. Hwang YH, Kim MK, Ahn SI. Consistency of Bruch membrane opening detection as determined by optical coherence tomography. *J Glaucoma*. 2016;25:873–878.
29. Pearce JG, Maddess T. Inter-visit test-retest variability of OCT in glaucoma. *Optom Vis Sci*. 2017;94:404–410.
30. Mansouri K, Weinreb RN, Liu JH. Effects of aging on 24-hour intraocular pressure measurements in sitting and supine body positions. *Invest Ophthalmol Vis Sci*. 2012;53:112–116.


Investigative Ophthalmology & Visual Science